JOURNAL OF MATERIALS SCIENCE 18 (1983) 2484–2496

The tearing of highly oriented linear polyethylene

J. CLEMENTS, I. M. WARD
Department of Physics, University of Leeds, Leeds, UK

The tearing behaviour of oriented linear polyethylene has been studied with particular emphasis on the effects of draw ratio, draw temperature and molecular weight distribution. In all cases the values of fracture surface energy were in the range 10^2 to 10^4 Jm^{-2}. The differences between the low molecular weight grades and high molecular weight grades of linear polyethylene were large. At high molecular weight the energy for crack propagation parallel to the direction of orientation fell by a factor of approximately two as the draw ratio was increased from 10 to 20. At low and medium molecular weights, increasing the draw ratio above a value of 10 had no significant effect on the fracture surface energy. Observation of the fracture surfaces showed a simple relationship between the nature of the fracture surface and the value of the fracture surface energy. In general, the higher the value of fracture surface energy the less fibrillar is the fracture surface. Furthermore the fibrillar nature of the fracture surface is essentially determined by the void content of the material.

1. Introduction

The mechanical anisotropy of oriented polymers has been well documented, and a number of studies have attempted to characterize the elastic behaviour in the small strain region [1–4]. The effect of anisotropy on the yield behaviour of semicrystalline polymers has also been extensively studied [5, 6]. In contrast, little has been reported on the anisotropic fracture properties of oriented semicrystalline polymers [7, 8].

The tearing properties of oriented films of polyethylene are of particular importance because of the potential application of such materials due to their very good gas barrier properties and chemical resistance. It is therefore of considerable interest to determine the key factors which influence the lateral strength of oriented polyethylene films.

In this paper an account is presented of measurements of the tearing energy of highly oriented linear polyethylene (LPE) and a polyethylene copolymer. The effects of molecular weight and draw temperature are examined.

2. Experimental details

2.1. Materials

Five grades of linear polyethylene homopolymer and one grade of copolymer were used in the present work. The molecular weight characteristics as supplied by the manufacturers are given in Table I.

2.2. Preparation of samples

2.2.1. Oriented sheets by tensile drawing

Sheets of isotropic linear polyethylene were prepared by compression moulding at 160° C and quenching in cold water. Full details of this process have been described by Capaccio and Ward and co-worker [9–11]. For one series of tests, specimens of dimensions 100 mm x 120 mm x 0.5 mm were then drawn in air at various temperatures (depending on molecular weight grade) at a crosshead speed of 100 mm min^{-1} in an Instron tensile testing machine. A grid printed on the sheet before drawing provided a measure of extension. The temperatures at which selected grades were drawn are given in Table II.

0022–2461/83 $03.00 + .12

TABLE I The molecular weight characteristics of the linear polyethylene grades used in all tests.

Grade	$\bar{M}_w$	$\bar{M}_n$	$\bar{M}_w/\bar{M}_n$
Homopolymers			
H020-54P*	312 000	33 000	9.45
Hizex 7000F†	318 000	15 100	21.05
Rigidex 9*	126 000	6 060	20.9
Rigidex 006-60*	135 000	25 500	5.29
Rigidex 50*	101 450	6 060	16.74
Copolymer			
002-055*	155 000	16 800	9.2

*BP Chemicals International Limited.
†Mitsui, Japan.

TABLE II The drawing temperature of selected LPE grades used in constant extension rate tests

Grade	Temperature (° C)
H020-54P	75, 115, 130
Rigidex 9	75, 95, 130
Hizex 7000F	115
002-55	115
006-60	75

For a second series of tests, dumb-bell specimens of gauge dimensions 20 mm x 5 mm were cut from these sheets and drawn in air at a cross-head speed of 100 mm min^{-1} on an Instron tensile testing machine. Draw ratios were measured from a series of ink dots marked on the undrawn dumb-bell gauge length. Draw temperatures used and final draw ratios are shown in Table III.

2.2.2. Oriented sheets by hydrostatic extrusion

It was recognized that the wide sheets prepared are drawn at constant width and are therefore likely to be of different structure to a sample drawn uniaxially. Uniaxial drawn sheets were therefore prepared following the split-billet technique originated by Porter and co-workers [12]. The method adopted was as follows: a solid cylindrical billet was machined from an isotropic rod prepared by an extrusion moulding technique [13], and carefully split across the diameter. A sheet of an identical grade of linear polyethylene, prepared by compression moulding, was then sandwiched in between the two halves of the billet and the whole assembly was hydrostatically extruded. The technique for hydrostatic extrusion of polymers has been described previously [13]. In the present work a conical die of 15° semi-angle was used, the final bore diameter being 15.5 mm. In extrusion we define the deformation ratio as the cross-sectional area of the billet divided by that of the product. All samples were extruded at 100° C.

2.3. Characterization of oriented sheets

The oriented sheets were characterized in terms of both their extension moduli and their wide angle X-ray diffraction patterns. The measurement of moduli were made by using the dead-loading creep apparatus described in a previous publication [4], the modulus being determined at a strain of 0.1% 10 sec after the application of the load.

Wide angle X-ray diffraction photographs were taken using an Enraf-Nonius X-ray generator employing nickel filtered Cu$K\alpha$ radiation and using wet film. The photographs showed that the

TABLE III The drawing temperatures, final draw ratios and representative values of G_c measured in constant load tearing tests

Grade	Draw temperature (° C)	Draw ratio	G_c(kJ m^{-2})
H020-54P	75	10	2.12
		17	0.64
	115	10	3.32
		20	1.88
Rigidex 9	75	8	1.48
		13.5	1.45
Rigidex 50	75	10	0.86
		15	0.84
002-55	115	10	0.90
		15	0.87
006-60	100	10.2	0.78
Split billet experiment		14.3	0.77

The values of G_c are those measured at an extension rate of 0.50 μm sec^{-1} in all cases.

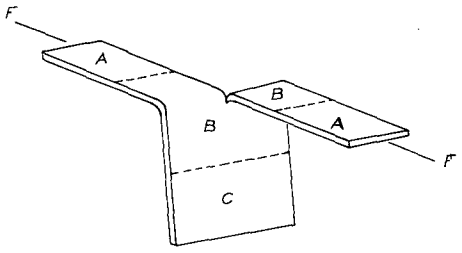

Figure 1 Trouser leg test specimen.

final samples possessed a high degree of orientation. The patterns for samples produced by tensile drawing of wide sheets show that the crystallographic *b*-axes are perpendicular to the *c*-axes but are in the plane of the sheet, whereas the *a*-axes are normal to the plane of the sheet. The lamellar texture of these samples is therefore similar to that of *b*–*c* sheet in low density polyethylene [14]. The patterns for samples produced by tensile drawing of narrow gauge dumb-bells and hydrostatic extrusion of wide sheets show fibre symmetry.

2.4. Fracture tests

The determination of the fracture properties of very thin sheets presents special problems of testing and analysis. The low lateral stiffness of thin oriented sheets means that conventional testing geometries, such as notched tension tests, are extremely difficult to use because of buckling. A test which overcomes this problem by exploiting the high flexibility of thin sheets is the trouser leg tearing test, which has been developed primarily for use on rubbers [15–17]. This geometry allows a tear to grow in a controlled fashion by separating the "legs" with a force F. Although tearing proceeds nominally in Mode III or "shearing mode", distortion of the test piece, particularly local to the tear front, can result in the tear proceeding in Mode I, or "opening mode".

Rivlin and Thomas [15] have analysed this test in detail and have modelled the situation as shown in Fig. 1 in which A is an area of specimen in simple tension at small strains, B is a highly deformed region and C is an undeformed region. As energy balance is set up and, provided the width of the sheet is sufficiently large, the elastic energy release in the "legs" is negligible compared with the work done by the applied forces F. If the energy per unit length of tear front is G_c, then the rate of external working is just sufficient to propagate the tear, i.e.

$$F\dot{x} = G_c H\dot{a} \tag{1}$$

where H is the sheet thickness, $\dot{a}$ is the rate at which the tear grows and $\dot{x}$ is the rate at which the forces separate.

2.5. Tearing at constant extension rate

If $\dot{x} = \dot{a}$, the rate at which the forces separate is identical to the rate at which the tear grows, then

$$F = G_c H \tag{2}$$

The tear in a rubber is in true plane strain, i.e. a flat fracture is produced with no plastic yielding, and G_c is a constant for all thicknesses of material.

The very simple result of Equation 2 expresses the fact that, since no significant amount of energy is stored in the bulk of the specimen, the whole of the work performed by the applied force is consumed in the tearing; tearing in this context consists of deformation of the material in the vicinity of the crack tip, and in the formation of the new surfaces.

2.6. Tearing at constant load

Equation 1 can also be used to describe a tearing test performed at constant load. Since $F\dot{x} = G_c H\dot{a}$ (Equation 1) then

$$\dot{a} \propto \dot{W} \tag{3}$$

where $\dot{a}$ is the tearing rate, the rate at which new surfaces are created, and $\dot{W}$ is the rate at which work is being done by the applied forces F.

2.7. Constant extension rate tests

For the constant extension rate tests the test pieces used were of rectangular shape, their length being not less than 50 mm and their width about 10 mm. An initial cut of about 20 mm was inserted along the centre line of the specimens by means of a razor blade whose edge was held perpendicular to the plane of the sheet and inserted from the end, i.e. in the direction of propagation, thus giving a sharp tip to the initial crack. The two free ends thus formed were clamped in the Instron jaws to give a test piece of the form shown in Fig. 1. The jaws were then separated at a rate of 25 mm min^{-1} and the resulting force–extension curve was recorded.

For measurement below room temperature an enclosure of rigid polyurethane foam was fitted around the test piece and Instron grips.

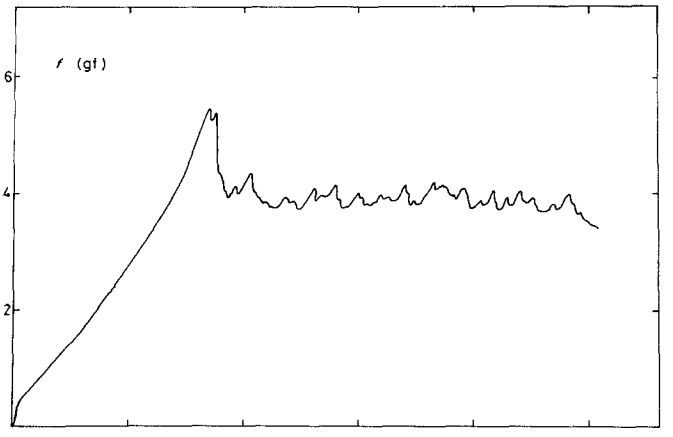

Figure 2 Tearing curve for Rigidex 9 of draw ratio 8.5.

The temperature inside the enclosure was controlled by a stream of cold nitrogen gas boiled off from a Dewar which passed over a heater into the enclosure. The relatively large volume of the enclosure meant that there was usually a significant temperature gradient. Hence, the effective temperature of the specimen is estimated to be accurate to only ± 3° C in every case.

2.8. Constant load tests

For the constant load tests the test pieces used were in the form of narrow tapes of rectangular shape, their length being not less than 80 mm and their width not less than 2 mm (depending on the final draw ratio). An initial cut of about 20 mm was inserted along the centre line of the test piece using a razor blade adopting an identical procedure to that described above. The two free ends of the specimen thus formed were clamped in the jaws of a dead loading creep apparatus described in a previous publication [4]. After allowing the test piece to stabilize in the machine for 10 to 15 min, the load was applied. Readings of sample extension were then taken at regular intervals.

2.9. Scanning electron microscopy

Fracture surfaces were observed by scanning electron microscopy (SEM). For this purpose the crack tip and surrounding material were cut from the torn specimen and mounted upon an aluminium stub. The sample was coated with a thin layer of silver (just sufficient to prevent charging up in the electron beam) by vacuum metallization in an Edwards Vacuum Coating unit. The sample was then viewed in a Cambridge Scanning Electron Microscope and micrographs of the crack tip and surrounding tear surfaces were recorded.

3. Results

3.1. Constant extension rate tests

For all the samples tested the force first increased to a high value, then dropped and oscillated about a constant value. Fig. 2 shows the curve for a sample of low molecular weight grade linear polyethylene drawn to a draw ratio of 8.5 at 75° C, which is typical of all samples. The high initial force is presumably required to convert the artificial crack induced by the razor blade, to a natural one of smaller radius associated with continuous crack propagation.

In a few cases the irregularity of the load extension curve was such that measurement of the tearing force became impossible. Such cases were therefore rejected.

The room temperature values of G_c for all samples tested in this way are shown in Table IV.

The results of the measurements below room temperature are shown in Fig. 3 for H020-54P grade. In spite of the relatively large scatter of the results, there is a clear and significant rise in the value of G_c in all cases. The results are summarized in Table V for all materials tested. The rise in the value of G_c is steady and continuous from room temperature to the lowest temperatures in all cases.

3.2. Constant load tests

For every sample tested the extension was extremely rapid at first, but then slowed down and became steady. Various extension–time curves are shown in Fig. 4 for different load levels.

Referring to Equation 3

$$\dot{W} \propto \dot{a}$$

we can obtain pairs of values of $\dot{W}$ and $\dot{a}$ from curves similar to those in Fig. 4. Since the tearing

TABLE IV The room temperature values of G_c measured at constant extension rate

Grade	Draw temperature (° C)	Draw ratio	G_c (kJ m^{-2})	Modulus, E (GPa)
H020-54P	75	7.2	2.23 ± 0.21	6.2
	115	7.6	2.28 ± 0.35	7.0
	130	7.1	2.28 ± 0.21	5.6
Rigidex	75	8.5	0.85 ± 0.15	6.9
	95	8.9	0.85 ± 0.18	6.7
	130	8.5	0.83 ± 0.19	4.2
Hizex 7000F	115	6.8	2.40 ± 0.15	5.0
002-55	115	7.7	1.7 ± 0.10	7.3
006-60	115	7.0	1.6 ± 0.10	5.4

rate diminishes as the tearing proceeds it would appear appropriate to measure the tearing rate at various intervals along the extension against time plots. We have chosen three points quite arbitrarily; 210 sec after loading, 450 sec after loading and 900 sec after loading, and have taken average values of extension which assume that the extension rate is varying in a linear manner.

The results of this procedure can be seen, for example in Fig. 5, where the various symbols refer to the measurement of extension rate at various times after loading. Here, the rate at which the external load is doing work is a unique function of the extension rate, and does not depend on the time after loading.

Results for samples of high molecular weight, H020-54P, drawn at 75° C are presented in Fig. 6.

In contradistinction to the above results, the results of an identical analysis of extension–time plots for samples of the lower molecular weight grade Rigidex 50 are shown in Fig. 7. At low rates of extension, pairs of values of $\dot{W}$ and $\dot{a}$ appear to be independent of the time after loading. At higher rates of extension this is no longer the case. Moreover, there appears to be little or no effect of draw ratio. Other low molecular weight grade homopolymers and the copolymer showed very similar behaviour.

From these tests, the relationship between the rate of doing work on the test piece $\dot{W}$, and the rate of tearing $\dot{a}$ can be calculated. From this relationship a characteristic energy for tearing, G_c, at a given rate of tearing $\dot{a}$, can be estimated. However, as was noted above, for samples of low molecular weight grades of homopolymer and of the copolymer there does not appear to be a unique relationship between $\dot{W}$ and $\dot{a}$. G_c is shown as a function of tearing rate in Figs. 8 to 11.

In Fig. 8, the dependence of G_c on draw ratio and draw temperature is quite explicit. In Figs. 9 to 11, the relationship between G_c and tearing rate is slightly more complicated. There is a dependence of G_c on loading time, i.e. how long after loading the measurements of extension rate and energy release rate were made. In the range of tearing rates where comparisons are possible, G_c is invariably larger at longer loading times, for any particular tearing rate.

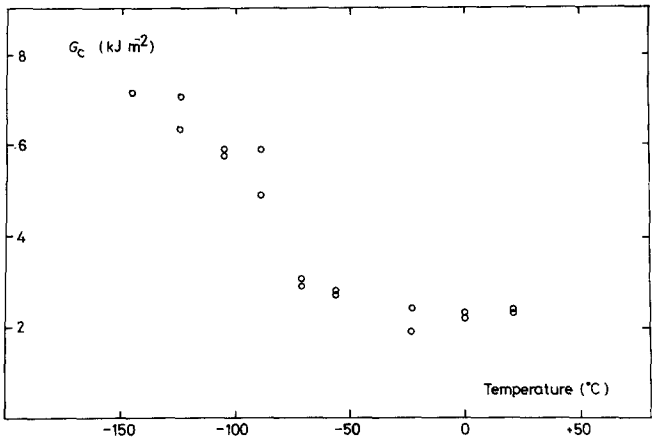

Figure 3 Fracture surface energy against temperature of test for H020-54P of draw ratio 7.6.

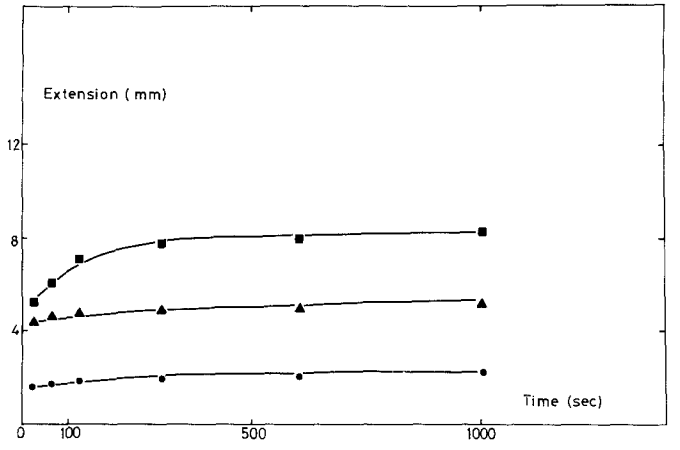

Figure 4 Extension against time plots for H020-54P of draw ratio 10: •, 30 g; ▲, 40 g; ■, 50 g.

3.3. Observation of fracture surfaces

Specimens of high molecular weight (H020-54P) drawn to draw ratio 10 at both 75 and 115° C, and of low molecular weight (Rigidex 50) drawn to draw ratio 10 at 75° C were torn in constant load extension tests. Material from the vicinity of the crack was then mounted and observed by SEM as outlined above. In all cases it was obvious that void formation preceded fracture. The crack was ill defined and measurement of crack tip diameters proved impossible.

Fig. 12 shows a typical void ahead of the crack tip in a specimen of low molecular weight. Several fibrils can be observed crossing the longitudinal void. Furthermore, the actual crack appears to have a multiplicity of tips. This is presumably due to void formation in a non-colinear fashion, i.e. voids forming on either side of the original crack axis, the centre line of the test piece. As the test proceeds these voids will become incorporated into the growing crack, and fibrils now cross the crack. These eventually rupture, and give rise to the observed irregularity of the fracture surfaces. The apparent multiplicity of crack tips is presumably due to the presence of strained but unruptured fibrils.

TABLE V The temperature variation of G_c measured at constant extension rate

Grade	G_c at room temperature (kJ m^{-2})	G_c at low temperature (kJ m^{-2})
H020-54P	~ 2.2	~ 7.2
Hizex 7000F	~ 2.4	~ 8.0
006-60	~ 1.6	~ 7.1
002-55	~ 1.7	~ 6.5
Rigidex 9	~ 0.8	~ 6.5

Fracture surfaces were observed for a variety of test pieces, tested in both types of tearing experiment, and are shown in Figs. 13 to 19. Comparing Figs. 13 to 16 and 17 to 19 we find that the two testing methods are indistinguishable in respect of fracture surfaces. Fracture surfaces were also observed for two samples tested at low temperatures, both high and low molecular weights, Figs. 20 and 21. The most noticeable feature is the absence of any significant fibrillar nature on the fracture surfaces.

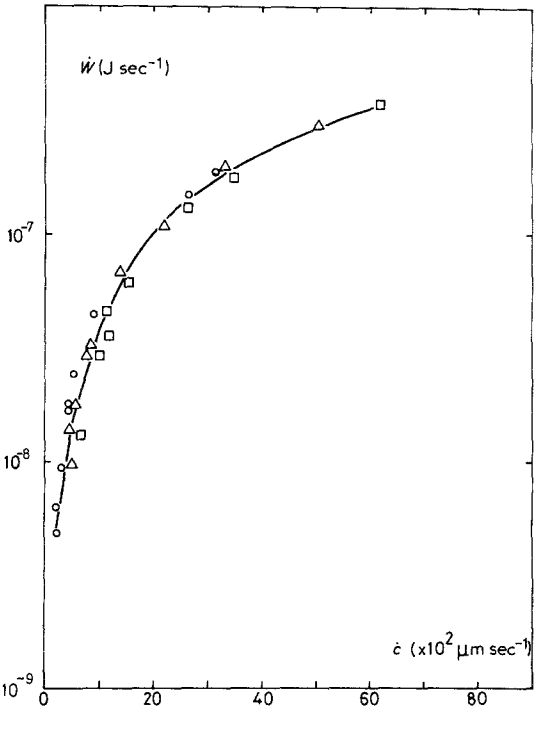

Figure 5 Energy release rate against extension rate for H020-54P, 115° C of draw ratio 10.

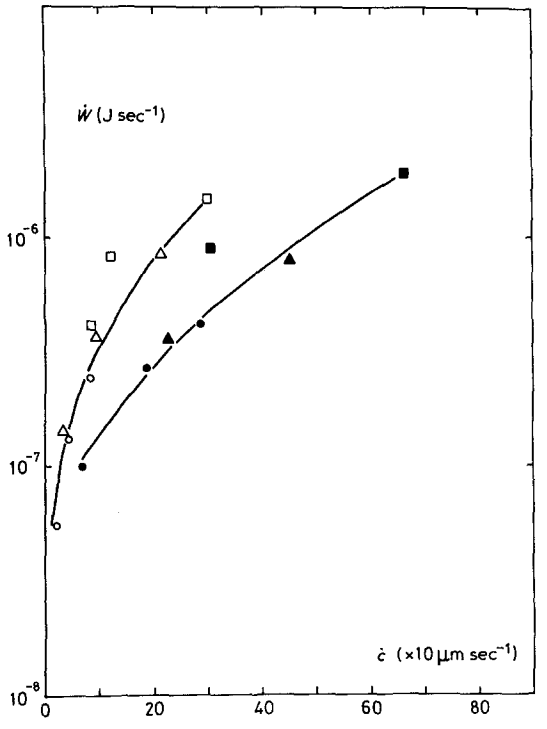

Figure 6 Energy release rate against extension rate for H020-54P drawn at 75° C: open symbols, draw ratio 10; and closed symbols, draw ratio 17.

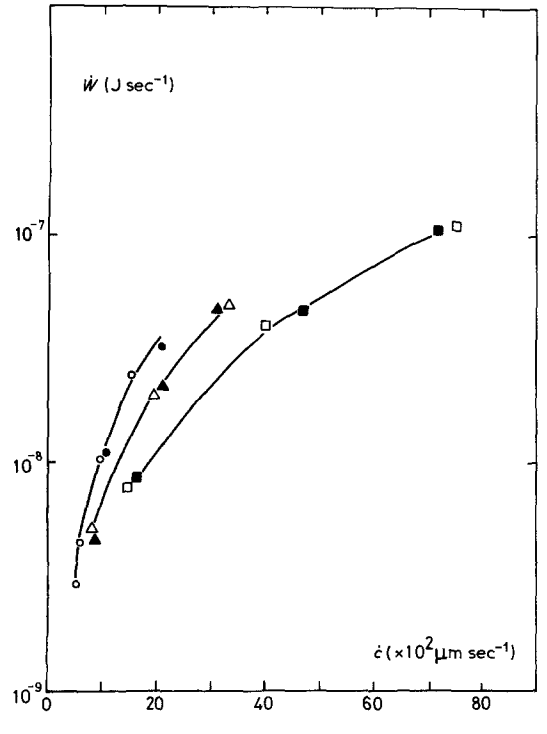

Figure 7 Energy release rate against extension rate for Rigidex 50 drawn at 75° C: open symbols, draw ratio 10; and closed symbols, draw ratio 14.

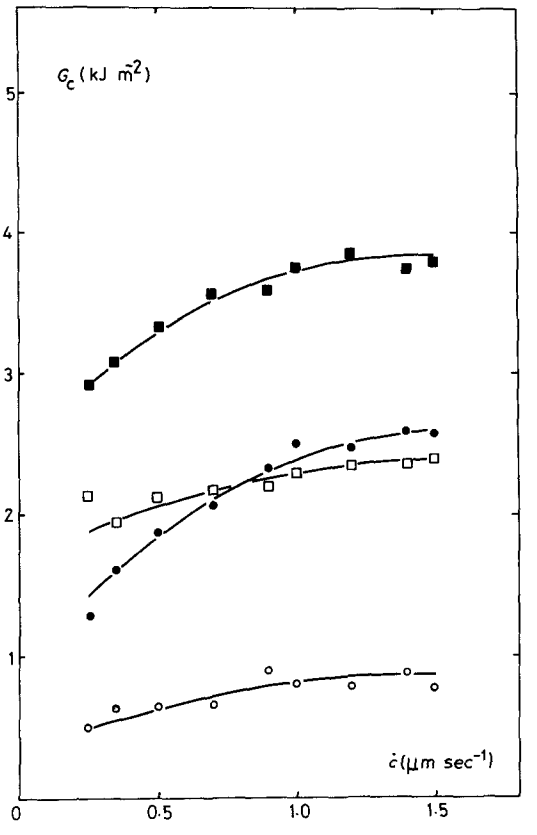

Figure 8 Fracture surface energy against extension rate for samples of H020-54P.

4. Discussion

In the present work, two methods have been employed for the characterization of the tearing properties of highly oriented linear polyethylene. Although a comparison of results from the two methods, constant extension rate and constant load, cannot be made directly, nevertheless some form of comparison is worthwhile. However, it must be borne in mind that the sets of samples used in each experiment are of somewhat different structure, those being used for constant extension rate tests are biaxially oriented (b–c sheets) while the samples used for constant load tests are uniaxially oriented (possessing fibre symmetry). In Table VI we present a comparison of room temperature values of G_c for two grades of homopolymer and the single grade of copolymer. Despite the enormous differences in extension rates at which the comparisons are made, and significant differences in draw ratio, there is still a very large measure of agreement between the two methods of testing. This agreement allows us to place some confidence in these results, and

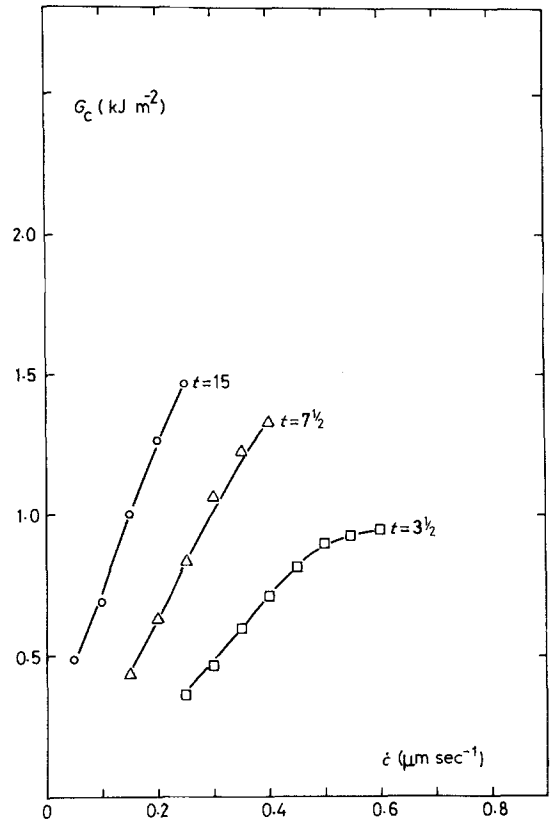

Figure 9 Fracture surface energy against extension rate for samples of 002-55.

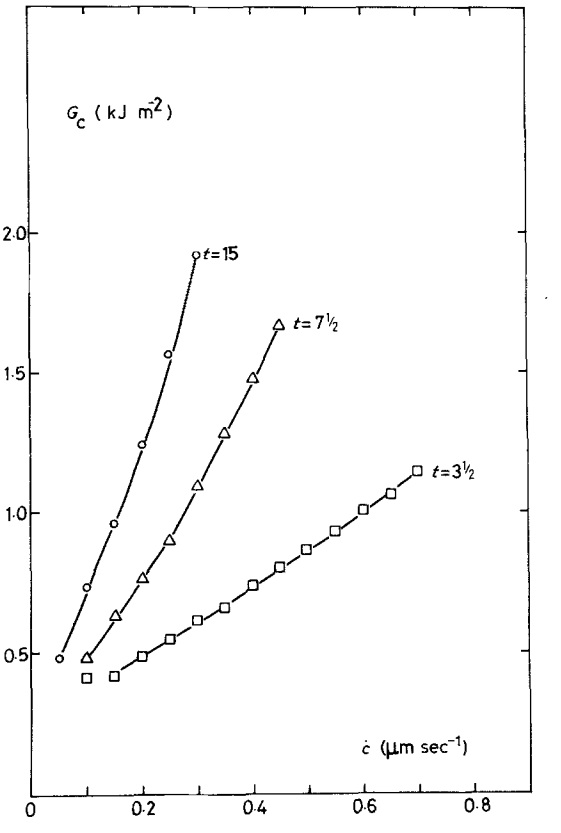

Figure 10 Fracture surface energy against extension rate for samples of Rigidex 50.

by extension, to those results where a comparison is not possible.

The reasons for measuring fracture surface energies on two different sets of samples in two distinctly different tests were twofold. Firstly, to extend the range of measurements to a wide range of draw ratios and molecular weight grades. Secondly, to work on samples which possess fibre symmetry, so that some degree of continuity could be established with previous work in this laboratory.

4.1. The effects of drawing on the fracture surface energy

In Table III we have tabulated values of G_c measured in constant load tearing tests. It is immediately obvious that only for samples of high molecular weight is there any dependence of G_c on draw ratio; at low molecular weights there is little or no variation of G_c. At first sight we might expect a decrease in the fracture surface energy with increasing draw ratio for all molecular weight

TABLE VI A comparison of room temperature values of G_c

Grade	Draw ratio	Draw temperature (° C)	Extension rate ($\times 10^6$ msec^{-1})	G_c (kJ m^{-2})	
H020-54P	7.2	75	416	2.23	CER
	7.6	115	416	2.28	CER
	10	75	0.5	2.12	CL
	10	115	0.5	3.32	CL
Rigidex 9	8.5	75	416	0.84	CER
	8	75	0.5	1.48	CL
002-55	7.7	115	416	1.7	CER
	10	115	0.5	0.9	CL

The abbreviations CL and CER refer to whether the measurement was undertaken at constant load or constant extension rate.

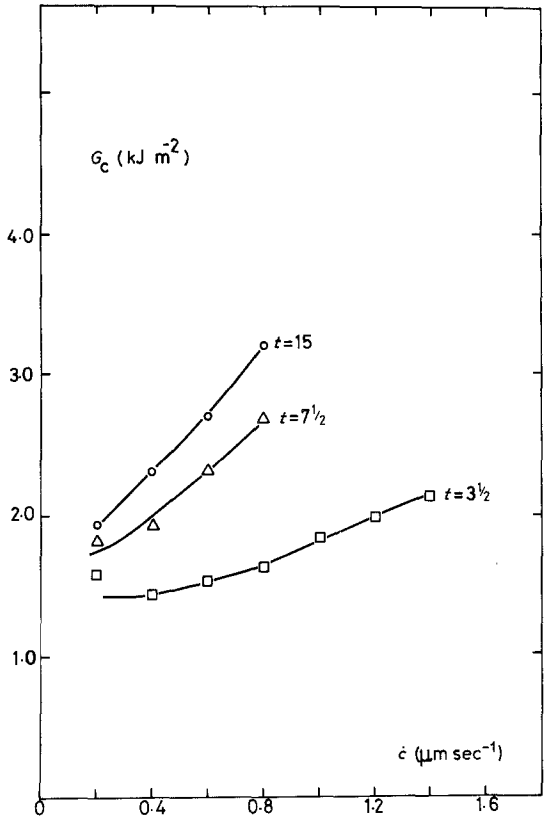

Figure 11 Fracture surface energy against extension rate for samples of Rigidex 9.

grades, due to preferential alignment of polymer molecules. Tearing parallel to the direction of preferential alignment requires the rupture of fewer and fewer bonds as orientation increases. However, the total contribution to the fracture surface energy from the rupture of bonds is negligible, when compared with the measured values of 10^3 to 10^4 J m^{-2}.

We propose that where a variation in the value of G_c is observed with increasing draw ratio, that this is due to variations in the amount of plastic work performed in the tearing process. The decrease in the amount of plastic work with increasing draw ratio is in turn due to changes in "lateral" morphology of the material which occur as drawing proceeds. At high molecular weights drawing produces changes not only within fibrils, but also between fibrils. At medium and low molecular weights, the fibrillar nature of the material is complete at relatively low draw ratios, and further drawing only produces changes within individual fibrils. These changes in *intra* fibrillar morphology have no bearing on the tearing properties.

An examination of the scanning electron micrographs shown in Figs. 13 to 19 clearly supports this proposition. In general, it would appear that lower fracture surface energies are associated with increasingly fibrillar fracture surfaces. Indeed, for samples of high molecular weight and low draw ratio there is virtually no fibrillation in evidence. As we noted above, fibrillar fracture surfaces are associated with the presence of longitudinal voids. The void content at medium and low molecular weights presumably does not change with increasing draw ratio. At high molecular weights, increasing draw ratio produces changes between fibrils, as well as within fibrils, and the morphological changes between fibrils are likely to produce voiding.

If we refer to Table III once more, the effect of specimen drawing temperature can be clearly seen. At comparable draw ratios, an increase in draw temperature significantly increases the value of G_c. Again we can propose that this variation

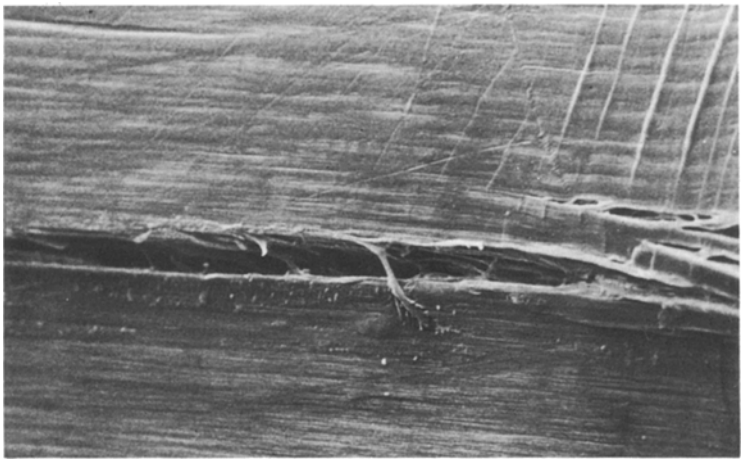

Figure 12 Micrograph of a void preceding the crack tip in an LPE specimen of low molecular weight.

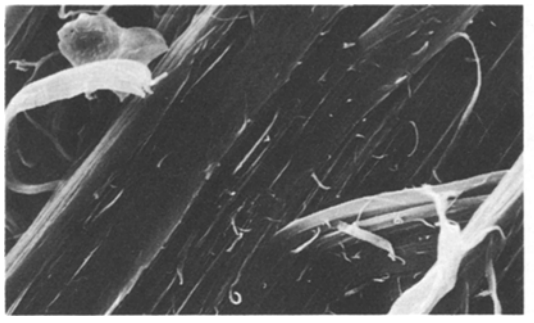

Figure 13 Micrograph of the fracture surface of high molecular weight LPE (H020-54P), draw ratio 10, draw temperature 75° C.

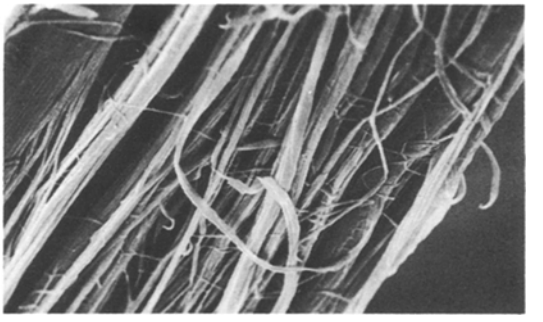

Figure 15 Micrograph of the fracture surface of high molecular weight LPE, draw ratio 17, draw temperature 75° C.

in the value of G_c is due to variations in the amount of plastic work performed in the tearing process. Furthermore, scanning electron micrographs support this proposition. Fig. 14 shows little evidence of any fibrillation on tearing of high molecular weight, low draw ratio, high draw temperature specimens. At higher draw temperatures the tendency to produce *inter* fibrillar voids is suppressed leading to smoother fracture surfaces and hence higher values of G_c.

These observations emphasize the importance of the molecular network at high molecular weight and high draw temperatures which has been suggested by previous research [18]. In effect the network holds the structure and thus prevents fibrillation. Hence the much higher values of G_c.

4.2. Copolymer and low molecular weight homopolymers

As we noted above there are two features of the results for the samples of copolymer and low molecular weight homopolymer which are worthy of special interest. Firstly, the absence of any significant draw ratio dependence which has been examined in the previous section. Secondly, the fracture surface energy is apparently dependent on loading time. This time dependence immediately suggests the presence of some viscoelastic effects. One possible cause of viscoelastic effects are what we shall name "molecular pull-out". Even in copolymers and low molecular weight homopolymers there must be some kind of molecular connectivity between individual fibrils, a basic molecular network. In high molecular weight homopolymers this molecular network is presumably more highly developed. We are suggesting that in low molecular weight homopolymers and copolymers that molecular pull-out occurs during fracture, and that molecular pull-out is a time dependent process. This pulling out of molecules is presumably a precursor of fibrillation. At high molecular weights the network is more highly developed, molecular pull-out is more difficult, and fracture occurs by molecular chain rupture leading to smoother fracture surfaces.

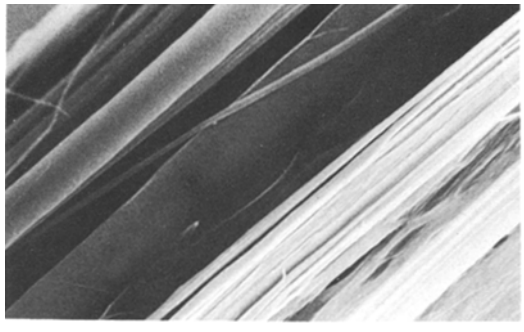

Figure 14 Micrograph of the fracture surface of high molecular weight LPE, draw ratio 10, draw temperature 115° C.

As an alternative to molecular chain pull-out we can propose that the increase in fracture surface energy with time is due to the presence of a strengthening structure at the crack tip. This strengthening structure takes an appreciable time to form and it seems not unreasonable to suggest that crystallization or something akin to it is responsible. This could be produced by the large deformation of the polymer in the neighbourhood of the crack tip. Crystallization at crack tips has been observed before, though only in rubbers, where it is responsible for the stick-slip behaviour upon tearing of gum vulcanizates and peroxide cured natural rubber vulcanizates [16].

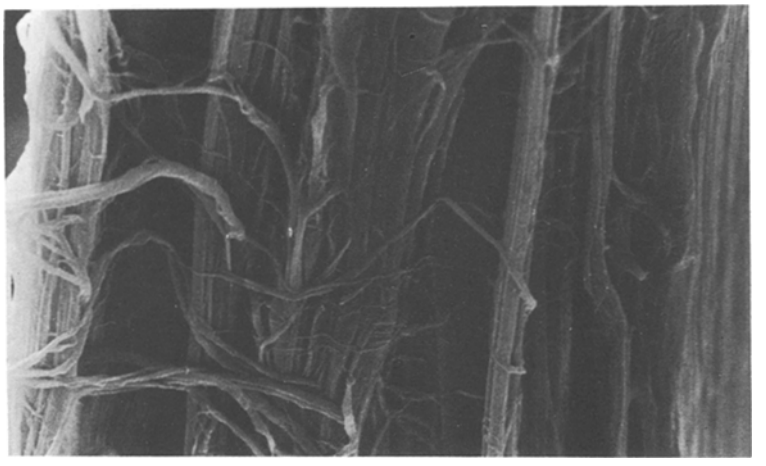

Figure 16 Micrograph of the fracture surface of low molecular weight LPE (Rigidex 50), draw ratio 10, draw temperature 75° C.

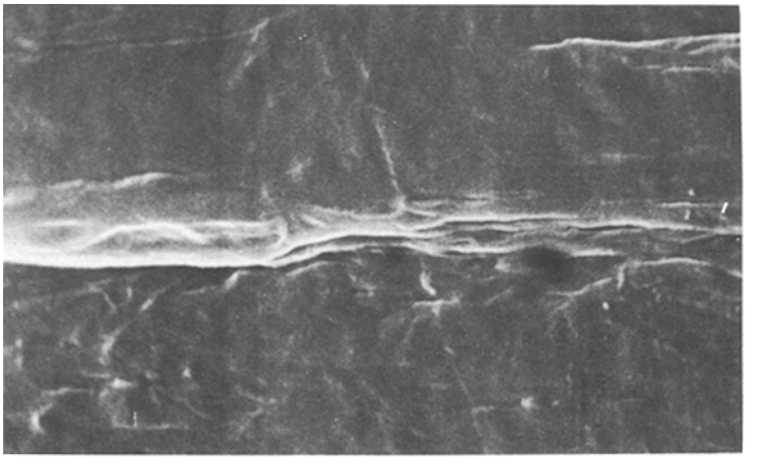

Figure 17 Void preceding crack tip in an LPE specimen of high molecular weight torn at constant extension rate.

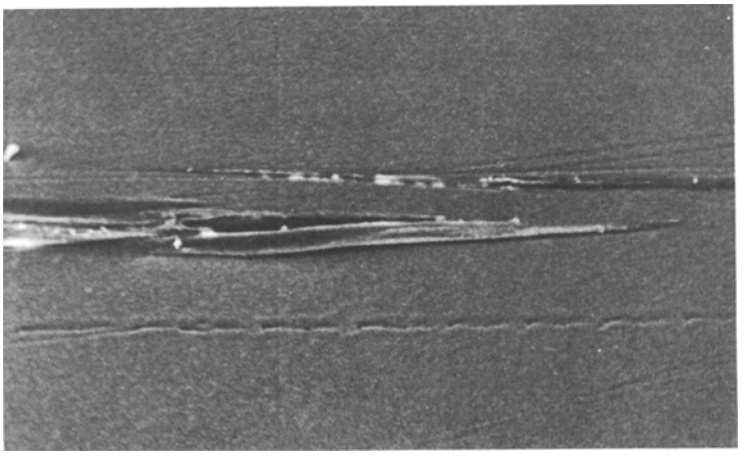

Figure 18 Void preceding crack tip in a specimen of copolymer torn at constant extension rate.

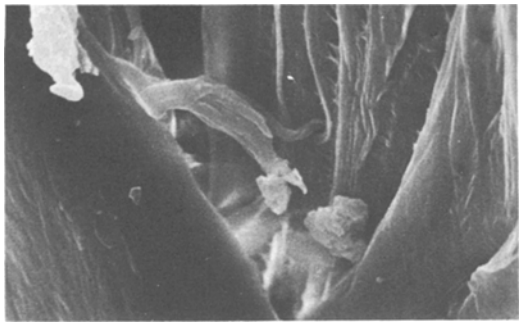

Figure 19 Fracture surface of high molecular weight LPW, draw ratio 7.6, draw temperature 115° C, torn at constant extension rate.

4.3. The temperature dependence of fracture surface energy

As we have seen in Fig. 3 and Table V there is a significant dependence of fracture surface energy on test temperature. All materials tested show a smooth continuous increase in G_c from room temperature to the lowest test temperature. The values of G_c for different polymer grades at the lowest temperatures show little variation; they are virtually all the same. The different polymer grades are all behaving in a similar way, despite the structural differences between them.

Scanning electron micrographs of low temperature fracture surfaces are shown in Figs. 20 and 21 for both high and low molecular weight homopolymers. There is very little evidence of fibrillation in either. This suggests that no molecular pull-out is occurring and that the network is retained, whatever its level of development. Fracture is presumably progressing through molecular chain rupture in every case.

5. Conclusions

The fracture surface energy of highly oriented linear polyethylene is of the order of 10^3 J m^{-2}.

The effect of increasing draw on the fracture surface energy is rather complex. At low and

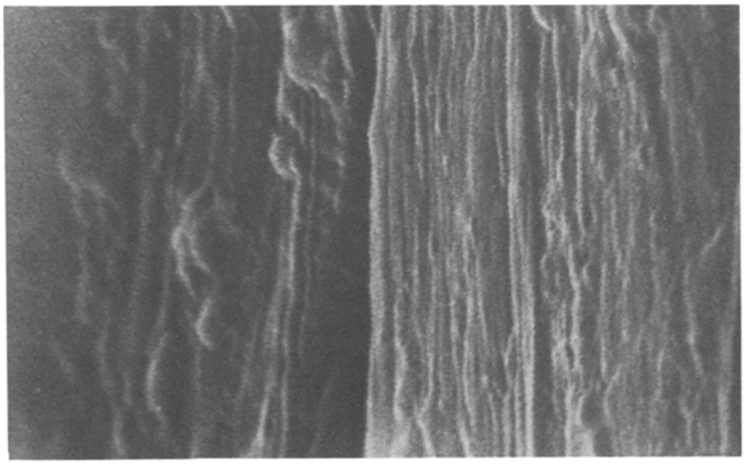

Figure 20 Fracture surface of high molecular weight LPE torn at constant extension rate at low temperature (– 150° C).

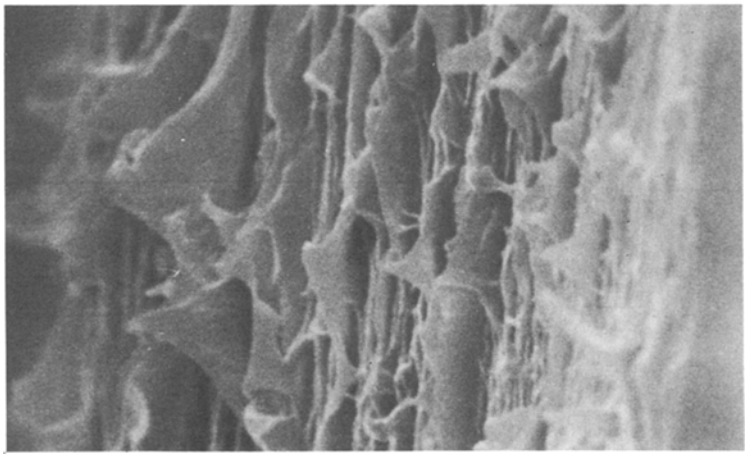

Figure 21 Fracture surface of low molecular weight LPE torn at constant extension rate at low temperature (– 150° C).

medium molecular weights, increasing draw ratio, above a value of 8 to 10, produces no significant effect on the value of G_c. At high molecular weights increasing draw ratio produces a dramatic reduction in G_c and it can fall to the level of that for low molecular weight materials.

The best prospects for production of oriented sheets of polyethylene with a reasonable resistance to tearing are obtained by drawing high molecular weight grades at high draw temperatures. The results which have been obtained emphasize the importance of retaining a molecular network in the drawn materials.

Acknowledgements

We are indebted to the Department of Textiles, the University of Leeds, and in particular to Dr M. G. Dobb and Mr T. Buckley for the use of the Scanning Electron Microscope, and to the Cookridge High Energy Lanoratory for irradiation of the samples.

References

1. G. RAUMANN and D. W. SAUNDERS, *Proc. Phys. Soc.* 77 (1961) 1028.
2. I. M. WARD, *ibid.* **80** (1962) 1176.
3. P. R. PINNOCK and I. M. WARD, *Brit. J. Appl. Phys.* **15** (1964) 1559.
4. V. B. GUPTA and I. M. WARD, *J. Macromol. Sci. Phys.* **B2** (1) (1968) 89.
5. A. KELLER and J. G. RIDER, *J. Mater. Sci.* **1** (1966) 389.
6. N. BROWN, R. A. DUCKETT and I. M. WARD, *Brit. J. Appl. Phys.* **1** (1968) 369.
7. G. E. ANDERTON and L. R. G. TRELOAR, *J. Mater. Sci.* **6** (1971) 562.
8. G. L. A. SIMS, *ibid.* **10** (1975) 647.
9. G. CAPACCIO and I. M. WARD, *Nature (London) Phys. Sci.* **243** (1973) 143.
10. *Idem, Polymer* **15** (1974) 233.
11. G. CAPACCIO, T. A. CROMPTON and I. M. WARD, *J. Polymer. Sci. Polym. Phys. Edn.* **14** (1976) 1641.
12. A. E. ZACHARIEDES, P. D. GRISWOLD and R. S. PORTER, *Polym. Eng. Sci.* **18** (1978) 861.
13. A. G. GIBSON, I. M. WARD, B. N. COLE and B. J. PARSONS, *J. Mater. Sci.* **9** (1974) 1193.
14. I. L. HAY and A. KELLER, *ibid.* **1** (1966) 41.
15. R. S. RIVLIN and A. G. THOMAS, *J. Polym. Sci.* **10** (1953) 291.
16. A. G. THOMAS, *ibid.* **18** (1955) 177.
17. H. W. GREENSMITH and A. G. THOMAS, *ibid.* **18** (1955) 189.
18. G. CAPACCIO, T. A. CROMPTON and I. M. WARD, *Polymer* **17** (1976) 644.

Received 29 December 1982
and accepted 20 January 1983